# Performance Evaluation of Fault Detection Algorithms as Applied to Automotive Localisation

Olivier Le Marchand, Philippe Bonnifait, Javier Bañez-Guzmán, François Peyret, David Betaille

# Performance Evaluation of Fault Detection Algorithms as Applied to Automotive Localisation

Olivier Le Marchand, *Renault SA, Guyancourt, France*
Philippe Bonnifait, *Heudiasyc UMR 6599, Université de Technologie de Compiègne (UTC), France*
Javier Ibañez-Guzmán, *Renault SA, Guyancourt, France*
François Peyret, *Laboratoire Central des Ponts et Chaussées (LCPC), Nantes, France*
David Bétaille, *Laboratoire Central des Ponts et Chaussées (LCPC), Nantes, France*

## BIOGRAPHY

**Olivier Le Marchand** obtained his engineering and master thesis in computer science from the University of Technology of Compiegne (UTC) in 2006. He is currently a second year PhD candidate on an industrial based thesis between Renault, UTC and the Laboratoire Central des Ponts et Chaussées (LCPC). His thesis addresses the estimation of position integrity of land platforms in urban environments.

**Philippe Bonnifait** is Professor at the UTC, computer science department. He graduated from the Ecole Superieure d'Electronique de l'Ouest, and received the PhD degree in Automatic Control and Computer Science from the Ecole Centrale de Nantes. In December 2005, he obtained the "Habilitation à Diriger des Recherches" from UTC. Since 1998, Ph. Bonnifait is with Heudiasyc UMR 6599, a joint research laboratory between the Centre National de la Recherche Scientifique (CNRS) and the UTC. His current research interests are in Robotics, Intelligent Vehicles and Advanced Driving Assistance Systems with particular emphasis on dynamic ego-localisation based on multisensor-fusion (GNSS, dead-reckoning and GIS).

**Javier Ibañez-Guzmán** obtained his PhD at the University of Reading on a SERC-UK assistantship and his MSEE at the University of Pennsylvania (USA) as a Fulbright scholar. He is currently working for Renault S.A where he is responsible for localisation technologies used in advanced driving assistance systems. Dr Ibañez-Guzmán has worked as senior scientist at SIMTECH, a national research institute in Singapore, where he spearheaded work on autonomous ground vehicles for unstructured environments. His research interests are in localisation and perception for vehicle guidance, and autonomous systems technologies.

**François Peyret** is graduate from the Ecole Nationale Supérieure de Mécanique et d'Aérotechnique of Poitiers and from the Ecole Nationale Supérieure de l'Aéronautique et de l'Espace of Toulouse. He is now Director of Research (equivalent of Professor), and head of the "Image processing and geopositioning" research team, at the LCPC, where he is leading research activities in the field of road vehicle positioning for ADAS, especially with hybrid GNSS systems enhanced 3D map-matching.

**David Bétaille** is a researcher in the Division for Metrology and Sensor Instrumentation of the LCPC, where his current activity relates to vehicles positioning by satellites systems combined with dead-reckoning and mapping, ADAS and in general road safety applications compose the research context of his lab. He received his PhD in 2004 for his investigations at University College London on phase multipath in kinematic GPS.

## ABSTRACT

A very important parameter to measure the quality of localisation systems is integrity in Global Navigation Satellite System (GNSS). Within this perspective, Integrity first considers the removal of outliers at the receiver level. It is typically monitored applying Fault Detection and Exclusion (FDE) algorithms. Then, integrity ensures a high probability bounded position error by computing protection levels. However, their performance depends very much on the faults characteristics and data redundancy which reflect the environment in which location estimates are made, and thus differ from scenario to scenario. After analyzing the specificities of GNSS based positioning in the automotive context, and the mechanism of the Receiver Autonomous Integrity Monitoring (RAIM) algorithm, a novel Kalman Filter based FDE algorithm is proposed in this paper. This is validated using hybrid simulation techniques based on real data from vehicle proprioceptive sensors and partially simulated GNSS data, where satellite configuration and faults characteristics can be controlled. The chosen scenario is that found in urban environments, representative of areas where localisation systems suffer many difficulties when mounted on land platforms. A comparison between the RAIM and the new algorithm is included.

## 1. INTRODUCTION

The availability of low cost GNSS receivers and communications technologies are providing new opportunities for mobile location dependent applications otherwise known as Location Based Services (LBS) across many industries. The current impact and potential of GNSS related technologies in the automotive domains is and will be very strong as demonstrated by the proliferation on the use of all types of car navigation systems. Further, future Intelligent

Transportation Systems (ITS) that represent the new set of transport related applications depend on two fundamental technologies: Localisation and Communications. Sample applications includes: fleet management, road tolling, emergency call, traffic regulation, pay per use insurance, etc. [1] [2].

Most applications depend on the degree of precision and accuracy expected from the localization systems used. Those in which the quality of location information is crucial address safety issues like in the case of advanced vehicle navigation. For most applications, the only sources of absolute location information are GNSS receivers. Thus, when land vehicles move in urban canyons; these receivers perform poorly due to occlusion of signals, multipaths, etc. In such conditions, precision and accuracy indicators are not sufficient to determine the confidence in GPS dependent localization data. That is, location estimates could be biased and errors occur, with insufficient information to know that this is occurring.

GNSS receivers (the GPS being the most widely used) provide today the primary source of location information for automotive applications where traveled distances are long. They provide in open sky conditions, precision and accuracy with an order of magnitude of around 10 m even with low cost receivers. However, when deployed in conditions where occlusion exists like in urban canyons, results are poor. Further, even when used in conjunction with other sensors such as odometers or inertial sensors, the expected precision and accuracy remains low. A major concern for safety related applications is the inability to neither identify the loss in performance and thus inform the user nor predict it. This constraints the use of GNSS dependent applications in safety related applications.

For this purpose the paper centres on the detection of faults from a land vehicle perspective. The approach originates on the use of concepts applied in the aviation sector for navigation purposes, in particular the definition of the Required Navigation Performance (RNP). This is used by the International Civil Aviation Organization (ICAO) to define the safe operation within a defined airspace, which evaluates and constrains the location related performances in terms of accuracy, integrity, continuity and availability [3]. They provide a quantifiable measurement for the quality of the location estimates.

For land applications, the most adapted would be integrity as it defines the measure of trust on the correctness of the information supplied by the total system. It includes a description on the ability of the system to provide timely warnings to the user when the system should not be used for the intended application. It is therefore regarded as the trust in the precision and accuracy of the position provided by the GNSS or the whole localisation system. This is a measure currently missing for critical LBS. It could allow for deciding if the position estimate provided to the application is reliable for its intended use, without risking placing for example the driver in a hazardous situation.

This paper proposes a new method to evaluate the performance of FDE algorithms used within localisation systems for automotive applications in particular urban areas. In the next section, the notion of Integrity is examined and formulated in an analytical manner. Section 3. presents FDE algorithms from an automotive perspective. A novel method to evaluate these algorithms is presented in Section 4.. This includes a comparison of the results from those from classical Receiver Autonomous Integrity Monitoring (RAIM) algorithms. In Section 5., the use of combined real and simulation data from an urban canyon like environment is used. It allows for the incorporation of different satellite faults. Section 6. concludes the paper, with regard to the feasibility of the proposed evaluation algorithms to the land vehicle context as well as the evaluation method proposed.

## 2. GNSS INTEGRITY: STATE OF THE ART

The measure of integrity for a GPS is very important because GPS noise and disturbances cannot be managed by broadcasted data or by the receiver alone, particularly for automotive applications. To address the issue, it is necessary to understand how the integrity process is checked in other application domains and to verify the manner in which protection levels are determined.

### 2.1. CONVENTIONAL PROBLEM FORMULATION

The main noise or disturbances on a pseudorange measurement can be described as [4]:

$$\begin{aligned} Pr = D + \Delta T_{sat} + \Delta T_{rcv} + \Delta T_{iono} + ... \\ \Delta T_{tropo} + \Delta T_{multipath} + \Delta t_{noise} \end{aligned} \quad (1)$$

- $Pr$ Measured pseudorange
- $R$ True distance
- $\Delta T_{sat}$ Satellite clock error
- $\Delta T_{rcv}$ Receiver clock error
- $\Delta T_{iono}$ Ionospheric delay
- $\Delta T_{tropo}$ Tropospheric delay
- $\Delta T_{multipath}$ Multipaths at the receiver level
- $\Delta t_{noise}$ Receiver measurement noise

These errors lead to increase the pseudorange values, which affect the final calculated position. A GPS when in standard operation assumes the following hypotheses: Ionospheric delay, tropospheric delay and the satellite clock offset are removed using broadcasted corrections. The receiver clock offset is an unknown variable. Receiver measurement noise is constant and can be pre-evaluated. In ideal conditions, there is no reflecting material near the receiver, so multipaths are null. If the system works under these hypotheses, it is considered as "fault free", leading to what is considered as a high integrity.

Integrity monitoring aims to verify that the system is working as intended, what means there is no deviation between the behavior of the expected system and its current response. This can arise only from a consequent error in

the correction parameters, or from the violation of any of the above hypothesis, such as a multipath or a significant growth of the receiver measurement error. This is called a "fault" when it occurs. Therefore, the first goal of an integrity monitor should be to check the presence of all possible faults with respect to the standard mechanism of the GPS. It can then provide a quantification of the integrity to the user, like for example the protection levels in the aerospace domain. The checking of faults is done "externally" via SBAS and "internally" via FDE. Then, the protection levels are calculated, as shown in Figure 1.

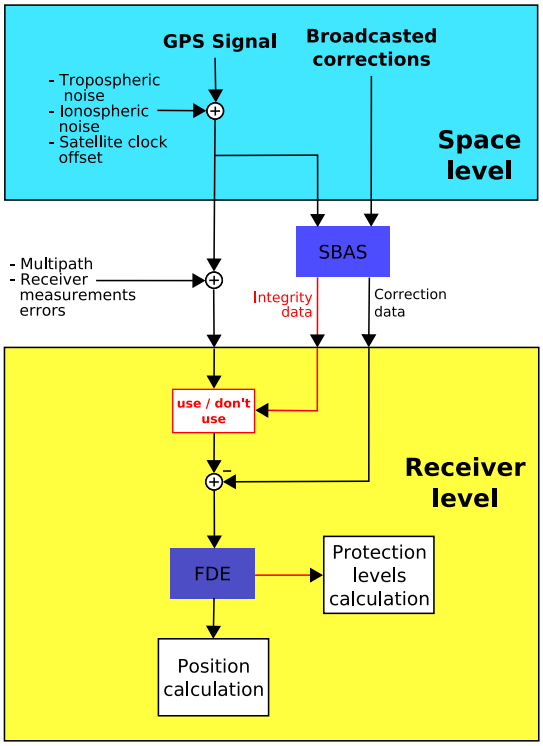


Figure 1: Fault checking through Integrity

## 2.2. SATELLITE BASED AUGMENTATION SYSTEMS (SBAS)

First, the integrity of GPS satellites and broadcasted data is performed by using information from Satellite Based Augmentation Systems (SBAS) such as EGNOS, WAAS and MSAS [5]. These continuously monitor the GPS satellites and broadcast a "use" / "don't use" information through geostationary satellites to all the GPS receivers within their area of coverage or via another communication medium. This is considered as a first level of trust in the location estimates. Moreover, SBAS have the ability to calculate better corrections and to broadcast them enhancing the GPS performance. As SBAS checks data independently of receiver data, it is called "external integrity".

## 2.3. FAULT DETECTION AND EXCLUSION (FDE)

Second, FDE algorithms must handle the remaining GPS faults, that is multipaths and receiver measurement errors [6][7]. For this purpose, the redundancy between the different pseudorange measurements is used. If all the measurements lead to a coherent position, no fault should be present. However, if an unexpected error appears on a pseudorange, this results in an oversized residual under some hypotheses.

The most well known FDE algorithm for GNSS receivers is the RAIM. Its principle is based on the use of a GNSS linearized equation that applies the least mean squares resolution:

$$d\rho = H.dX + \beta \tag{2}$$

where $d\rho$ is linearized pseudoranges vector. The noise $\beta$ on the pseudoranges is supposed to be independent, Gaussian and zero mean with known variances, and it is stored in a diagonal matrix denoted $Q\rho$, $H$ is the Jacobian of the observation matrix at the linearization point $dX$. The estimated linearized state is given by:

$$d\hat{X} = \left(H^T Q_\rho^{-1} H\right)^{-1} H Q_\rho^{-1} \cdot d\rho \hat{=} H^+ \cdot d\rho \tag{3}$$

where $H^+$ is the weighted pseudo inverse of matrix $H$. The residuals $\varepsilon$ can be calculated as the difference between the measured pseudorange and the "estimated pseudoranges"; these are derived from the estimated state:

$$\varepsilon = d\rho - H d\hat{X} = (I - HH^+) d\rho \hat{=} S \cdot d\rho \tag{4}$$

As matrix $S$ is idempotent, it cannot be inverted. Let denote $E$ a vector containing faults. $E(i) = b_i$ corresponds to a fault on measurement $i$, with an amplitude equals to $b_i$.

$$\varepsilon = S \cdot (d\rho + E) \tag{5}$$

If no fault is present, then $E = 0$, the residuals have zero mean since the variable $d\rho$ belongs to the Kernel of matrix $S$. If a fault occurs on a pseudorange, i.e. one element of $E$ is non-zero, then the residuals vector is no more centered. In practice, the detection is made thanks to the calculation of the Sum of the Squared Error (SSE), that is:

$$SSE = \varepsilon^T Q_\rho^{-1} \varepsilon \tag{6}$$

which is compared to a $\chi^2$distribution at $n-4$ degrees of freedom having a defined probability of false alarm, where $n$ is the number of satellites used. So an integrity failure is detected if:

$$SSE > \chi^2_{(1-P_{fa},n-4)} \tag{7}$$

Once the occurrence of a fault is detected, it is necessary to identify the faulty satellite in order to remove its measure from the calculation. A typical detection technique consists in computing a score $w_j$ for each satellite as function of its residual and its variance:

$$Q_\varepsilon = Q_\rho - H\left(H^T Q_\rho^{-1} H\right)^{-1} H^T \tag{8}$$

$$w_j = \left| \frac{\varepsilon_j}{\sqrt{(Q_\varepsilon)_{j,j}}} \right| \tag{9}$$

The maximum score indicates the faulty satellite. Once a satellite is identified, it is removed from the measurements, a new position is calculated, then a new detection test is performed and so on.

The following remarks are made with regard to this algorithm: First, from a practical point view, the more measurements and redundancy you have, the easier you detect a fault. In fact, the numerous healthy measures provide an estimated position with a low bias from which the faulty measurement clearly differs. Second, from a mathematical point of view, if the whole fault vector $E$ belongs to the kernel of $H$, it leads to a biased position whose residuals are zero mean, then faults are undetectable [8]. Thus, it can be assumed that the occurrence of several biases lead to a partial and mutual "compensation" which decreases the detectability of each bias through the residuals. Even if the probability of such event is very low, it can occur theoretically. This focuses on the key assumption of the RAIM: the hypotheses of only one fault occurring at a time, which is the main drawback of this algorithm when applied to the automotive context.

### 2.4. COMPUTATION OF THE PROTECTION ZONE

Once the possible faults are detected and excluded from the computation, the protection level is calculated. This depends on the computations of the FDE and on the data coming from the SBAS. For example, the HPL is often calculated as (c.f. [9]):

$$HPL = HSlope_{MAX}.Th + U(P_{md}) \tag{10}$$

If a fault occurred only on the pseudorange of the i$^{th}$ satellite, with a magnitude equal to $Err_i$, then the error in the horizontal plane will be equal to $HSlope_i \times Err_i$. So $HSlope_{MAX}$ represents the maximum $HSlope_i$ over all the satellites. Under the assumptions of only one fault at a time and of having a Gaussian noise of known variance on all the measurements, a threshold $Th$ can be determined according to a probability of false alarm and the satellite configuration. Finally, the solution spread due to the noise is taken in account through a conservative function $U$ depending on the probability of missed detection $P_{md}$.

The calculation of the $HSlope_i$ and of the $Th$ relies on similar equations to those in the FDE algorithm. Therefore, it will be submitted to the same problems. The lack of redundancy between measurements leads to an increase of both $HSlope_{MAX}$ and $Th$ what means an increase of the protection level. Further a hypothesis of always "one fault at a time" is assumed. Therefore, the protection level calculation is subject to the same limitation as the RAIM algorithm.

## 3. FDE FOR AUTOMOTIVE CONDITIONS

The previous section has presented a general approach to the GPS integrity problem. It is suitable for some context such as the aerospace domain for example. However, the automotive context is submitted to specific constraints, which deteriorate the performance of RAIM. Theses constraints are detailed thereafter and a new FDE algorithm is proposed.

### 3.1. THE INTEGRITY PROBLEM

The monitoring of GPS position estimates using a GPS receiver onboard of a car needs to take into account the environment traversed by the vehicle. Unlike aerospace applications, where vehicles travel on open skies, passenger cars traverse dense urban areas where GPS signals are shadowed and there is often the presence of multipaths. GPS signals are insufficient and thus a combination of proprioceptive sensors and vehicle models is used to ameliorate estimations. It is necessary to consider them in any analysis.

The focus in this paper is on Urban Environments, as these represent the most challenges and the needs for precise positioning in safety related applications identified. In an urban area where the streets are lined of buildings it is difficult to obtain more than 7 satellites and it is often less, when at least 8 or 9 are available in open sky view [7]. This context restrains the redundancy between the pseudorange measurements. Therefore the performance of conventional FDE algorithms decreases. In addition, the number of simultaneous faults and their frequency is significantly higher in urban than in rural areas. In this context, signal reflections from the built-environment are very high, leading to several simultaneous multipaths. Experimental data recorded of a vehicle travelling in such conditions (c.f. Figure 2) demonstrates this argument. A sample of the residuals obtained is shown in Figure 3. The experimental set-up consisted of an automotive low-cost type receiver mounted on a passenger vehicle. Despite the residuals are not fully representative of the faults due to the use of the least square estimation, the presence of simultaneous multipaths is highly probable.

Currently, mobile communications technologies allow for the availability of SBAS corrections in passenger vehicles. SiSnet is one example of EGNOS message availability through the Internet. Assisted GPS (AGPS) systems propose similar corrections as provided by GPS manufacturers or third parties. It can be argued that the integrity of the satellite level of the GPS system does not present specific problems for automotive type applications.

There is much work on the location estimation of car-like vehicles. The fusion of GPS, exteroceptive and proprioceptive sensors is the classical approach used to enhance precision and accuracy of the estimations [10][11][12]. The sensors used include wheel speed sensors (WSS), inertial sensors, video cameras, scanning lasers, etc. The solutions found in current passenger vehicle include WSS from ABS, and when available inertial related data from Electronic Stability Program (ESP), yaw rate gyroscopes, lon-

Figure 2: Representative picture of urban test area

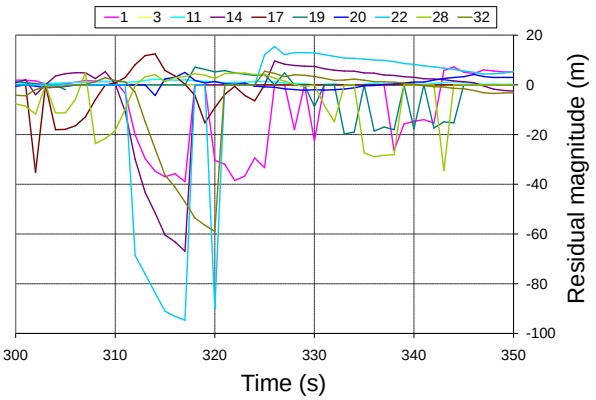


Figure 3: Pseudorange residuals on each satellite during an urban test

gitudinal and transverse accelerometers. The algorithms use different car motion models to combine data measured by these sensors. In this context, FDE algorithms must take advantage of these data, in particular through the use of direct measurements on the vehicle response and its relationship with the ground, like in the case of proprioceptive sensors.

### 3.2. ENHANCED FDE WITH PROPRIOCEPTIVE SENSORS

Due to the very specific environment traversed by the vehicles, the conventional FDE algorithms are not suited to automotive integrity monitoring. These can be improved by including information to what occurs with the platform to which the receiver are attached, that is the use of proprioceptive vehicle data (the vehicle ego-state). Such a solution is proposed in the following algorithm that makes use of this information associated by a Kalman filter.

Information from the prediction step of a Kalman filter helps to obtain a more accurate position, and thus more relevant residuals, as proposed in [2] and a variant can be found in [13] and [14]. To implement a tightly coupled Extended Kalman Filter (EKF) between GPS pseudoranges, WSS and a yaw rate gyroscope, the following state space system representation is used:

$$\begin{cases} X_{k+1} = f\left(X_k\right) \\ Y_k = g\left(X_k\right) + E \end{cases} \tag{11}$$

$$X = \begin{bmatrix} x & y & z & cdt & v & \omega & \theta \end{bmatrix}^T \tag{12}$$

$$Y = \begin{bmatrix} \rho^T & v_{lw} & v_{rw} & \omega \end{bmatrix}^T \tag{13}$$

where: $x$, $y$, $z$ are the coordinates in a local reference frame, $cdt$ is the bias in metres due to the clock offset, $\theta$ is the vehicle heading with respect to $x$, $v$ its velocity, $\omega$ its yaw rate, $v_{rw}$ and $v_{lw}$ the rear right and left linear speeds of the wheels. $f$ is a simple evolution model for a car vehicle moving in a navigation frame tangent to the earth, and $g$ the suitable observation function. The equations of the EKF estimation step are:

$$C_k = \frac{\partial g}{\partial X}\left(\hat{X}_{k+1|k}\right) \tag{14}$$

$$K_{\mathrm{k}} = P_{k+1|k}.C_k^T.\left(C_k.P_{k+1|k}.C_k^T\right)^{-1} \tag{15}$$

$$\hat{X}_{k+1} = \hat{X}_{k+1|k} + K_{\mathrm{k}}.\left(Y_k - g\left(\hat{X}_{k+1|k}\right)\right) \tag{16}$$

where $C_k$ is the Jacobian of the observation model, $P_{k+1|k}$ the covariance matrix of the predicted state and $K_k$ the Kalman gain. $C_k$ and $P_{k+1|k}$ can be represented as bloc matrices, where the GPS part and the proprioceptive sensors part can be partitioned:

$$C_k = \begin{bmatrix} H_k & 0_{n,3} \\ 0_{3,4} & \begin{bmatrix} 0 & 1 & -l/2 \\ 0 & 1 & l/2 \\ 0 & 0 & 1 \end{bmatrix} \end{bmatrix} \tag{17}$$

$$P_{k+1|k} = \begin{bmatrix} P_{GPS} & P_2 \\ P_3 & P_4 \end{bmatrix} \tag{18}$$

where $l$ is the wheel-track, $H_k$ is the $n$ lines, 4 columns matrix corresponding to the Jacobian of a GPS observation matrix, and $P_{GPS}$ the $n$ lines 4 columns upper left matrix which holds the covariance of the predicted position and $cdt$. The predicted position is used to calculate the residuals from the innovation of the EKF:

$$\varepsilon = \rho + E - h\left(\hat{X}_{k+1|k}\right) \tag{19}$$

Then the covariance of the residuals $P_\varepsilon$ must be calculated to normalize the residuals and calculate the new SSE:

$$P_\varepsilon = Q_\rho + H_k P_{GPS} H_k^T \tag{20}$$

$$SSE = \varepsilon^T P_\varepsilon^{-1} \varepsilon \tag{21}$$

The detection and identification steps present two major differences. The position is not estimated from the pseudoranges, it comes from the predicted step of the Kalman Filter. Consequently the number of degrees of freedom is equal to $n$. Thus the SSE is compared to a $\chi^2$distribution with n degrees of freedom:

$$SSE > \chi^2_{(1-P_{fa},n)} \tag{22}$$

Theoretically, this increases the detectability of this algorithm, and allows fault detection and identification on a constellation with less than 5 satellites. This is followed by the identification step performed by choosing the satellite with the highest normalized residual, with respect to $P_\varepsilon$.

The gain of this algorithm lies in the relevance of the residuals. In contrast to the residuals derived from least mean squares, the estimation state is not corrupted by the faults when they occurred at the first time. The idempotent matrix $S$ is not involved here, thus the impact of the fault vector $E$ is not weakened into the residuals. This should allow detecting faults as soon as they occurred. On the contrary, an undetected fault could maybe bias the state, what decreases the detectability of upcoming faults.

The second main advantage of this algorithm is the use of the covariance of the predicted state. The precision of the predicted state can be higher than the position precision obtained with a mean least squares solver, depending on the satellite configuration and the noise on the pseudoranges. Although this precision is used in the residuals normalization and has a role in the detection power, so a better precision can help to detect faults with lower amplitude.

## 4. A NEW METHOD TO TEST FDE

The previous sections have highlighted the interest of analyzing the performance of FDE algorithms. Such study includes numerous parameters having a major role in the results. Six faults and errors sources have been previously identified regarding to GPS systems, and two others parameters can be taken in account. The satellite constellation has a great effect on detectability. The receiver is moving, so the trajectory has its own effect if it is used in the filtering process. Such an analysis can be performed by several means, but the most probable ones are pure simulation and real tests, which are both inappropriate.

In the first case, the number of parameters involved in the simulation will certainly leads to an exponential complexity. Thus, the choice of the different values of the parameters is complex, and finally questions the validity of the results regarding to reality. The interpretation of the results is hardened by the complexity of the simulation too. For these two reasons, a pure simulation seems to be difficult to carry out and to explain. In the second case, real tests are hard to prepare for many reasons. The evaluation of FDE performances needs to detect the faults and to estimate their magnitude with enough precision via ground truth equipment. This can be easily realized for a fix receiver, but it is more complex with a mobile one. Moreover, the occurrence of faults is highly constrained by the environmental context, and it is not possible to control it enough in order to obtain predetermined faults. Thus, any test campaign seems unable to be exhaustive with respect to the diversity of possible faults. Consequently, real tests are not relevant to provide such performance analysis.

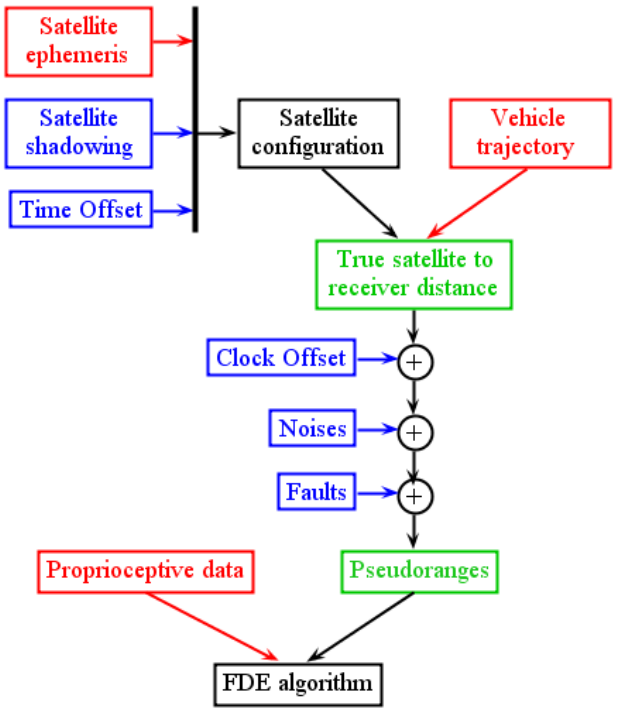


Figure 4: Evaluation method scheme

As a result, we propose to use real data enhanced by simulated ones in order to obtain a realistic and flexible test. The idea, schemed in Figure 4, is to use real data (in red) for complex parameters to set regarding to their low effects and to keep flexibility on the GPS signal part with simulated data (in blue). Thus, the trajectory of the vehicle comes from real records realized in an urban track in order to avoid the simulation of vehicle dynamic and of an urban path. This trajectory includes various urban dynamics: straight lines, roundabout, 90° turns, and slow curves. The same record is used to extract data from proprioceptive sensors, such as wheel speed sensor and a yaw rate sensor. Finally, the satellites positions are extracted from GPS broadcasted ephemeris. On the other side, satellite shadowing, time offset on ephemeris, clock offsets, noise and faults are defined as parameters of the simulated data in the purpose of maximizing the performance evaluation. Because the values of these parameters are not clear, it is detailed in the next section.

### 4.1. PARAMETERS SET

Let recall that our tests focus on FDE algorithm performance in an automotive context, what means that the most interesting fault source is multipath. Other sources of noises have to be included but should not introduce faults. The satellite configuration has to be controlled as it influences the redundancy too. Finally the properties of multipath faults have to be well-defined.

As expressed by equation (1), the GPS signal is submitted to ionospheric and tropospheric delays, which increase the pseudoranges. These noises are highly complex to model. Because they are not the main purpose of this test, it has been decided to assume that the GPS receiver is able to get corrections. Even if they are not total, it is assumed the remaining error is insignificant with respect to the magnitude of the faults we focus on.

The clock offset error and the receiver measurement noise are highly dependent on the device used, and cannot be modeled in a generic manner. In order to simulate them, a reference receiver has been chosen and recorded to extract relevant parameters. Because the test is dedicated to automotive context with low cost receiver, it has been decided to use an Ublox Antaris 4 GPS receiver. As the measurement noise has to be observed through raw data, a LEA-4T model has been used for the experiment. In order to model the evolution of the clock offset, a static record on an open sky view site has been performed during 2 hours. The clock offset, plotted in Figure 5, was included between +6ms and -8ms, and the clock drift is plotted in Figure 6. Thus, the clock bias is simulated with a linear evolution and we suppose that no jump occurs during the simulation.

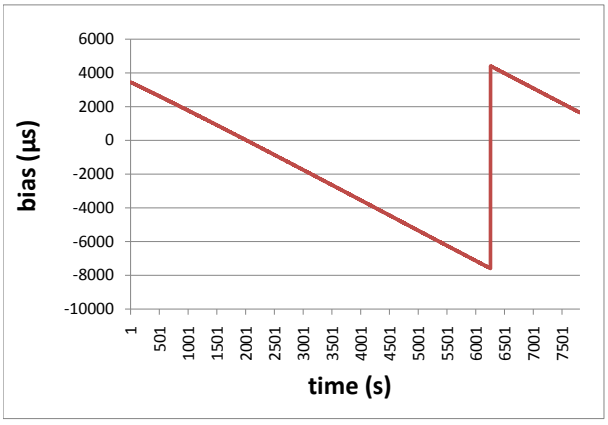


Figure 5: Ublox LEA-4T clock bias

The same record was used to quantify the noise measurement of the receiver. With the help of a fix receiver part of the French "Réseau GPS permanent" (RGP), simple differences have been performed in order to remove ionospheric and tropospheric noise. Knowing the exact position of the receiver, the receiver clock offset and assuming the absence of multipaths, the measurement noise can be observed. The observation of this noise shows it is not a Gaussian noise, and its magnitude is a function of the satellite elevation. It has been decided to model the noise color

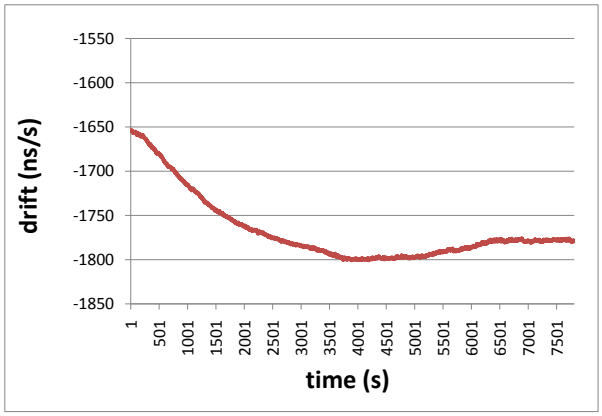


Figure 6: Ublox LEA-4T clock drift

by a shaping filter based on a second order autoregressive model:

$$F(z) = \frac{1}{z^2 - a.z - b} \tag{23}$$

As mentioned above, the satellite configuration determines the redundancy of the measurements on which FDE algorithms are based. Consequently, it is interesting to study the effect of the number of satellites on the FDE performances. Moreover, this should be analyzed under various satellite configurations in order to be representative. The specificity of the urban context should not be forgotten, and two main issues have to be taken in account: 1) The number of satellites in direct view rarely exceeds 8 satellites. 2) The satellites with a high elevation have more chances to be in view. As a result, the tests are always performed with the highest satellites, and their number is between 3 and 8. Even if detection and exclusion with RAIM cannot be performed with less than 6 satellites, it is interesting to see how faults can be detected with the algorithm using proprioceptive data. The constellation diversity is obtained by shifting a time offset on the ephemeris file on a one-day period with a half an hour incremental step between two tracks.

Finally, the parameters of the multipaths have to be defined. Three parameters are fundamental: the magnitude of the faults, the number of simultaneous faults and their duration. Because a full study on multipath occurrence for urban environment on moving vehicle with low-cost receiver has not been performed yet, we base our parameter setting on the residuals observation of the Ublox Antaris 4 during an urban track test. The residuals on all the satellites have been recorded in urban area as shown in Figure 3, where the residual is set to zero when the satellite is not used to calculate the position. Despite the residuals are not fully representative of the faults because of the least squares estimation, they give information about the number of simultaneous faults and an order of magnitude about their amplitude and duration. Thus, we can assume that more than 3 multipaths can occur at the same time. The amplitude of the multipaths can reach 80 meters, with minimum ampli-

tude approximately equal to 10 meters. The duration seems to vary between 1 and 10 seconds maximum.

Consequently bias of 15, 30 and 45 meters have been added on the pseudoranges during the test tracks, always at the same moment for all the satellite configurations. Regarding to the number of satellites used, 1, 2 or 3 simultaneous biases of the same amplitude are introduced and all the combinations between the visible satellites are tested. The false alarm rate for the $\chi^2$test has been set to 0.1%, in order to highlight the performance differences between both algorithms.

The choice of all mentioned parameters is inevitably arbitrary, but it focuses on realist parameters, where FDE algorithms should be able to work efficiently. Indeed, it is difficult to consider every combination of all the parameters.

## 5. RESULTS

This section presents the results obtained for both algorithms, with exactly the same GPS data and the same detection parameters. The performance of the usual RAIM algorithm is first analyzed with respect to its detection and identification abilities. Then, the same analysis is performed for the Kalman filter based FDE.

### 5.1. RAIM

The false detection rate, shown in Table 1, represents the percentage of times a fault was detected, i.e. the SSE has exceeded the $\chi^2$threshold, whereas no fault was introduced in the simulation. The difference between the false alarm rate set up in the simulation and the results arises from the non-white noise on the pseudoranges. It has been verified that running the simulation with Gaussian noise leads to a coherent false detection rate. Since false detections occur in the absence of any fault, the false detection rate is independent of the bias amplitude.

| Bias amplitude | Number of Satellites | | | |
|---|---|---|---|---|
| | 8 | 7 | 6 | 5 |
| 15 m | 0.00% | 0.00% | 0.02% | 0.13% |
| 30 m | 0.00% | 0.00% | 0.02% | 0.13% |
| 45 m | 0.00% | 0.00% | 0.02% | 0.13% |

Table 1: False Detection rate of the RAIM algorithm with one fault

Table 2 and Table 3 show the Missed Detection rate, i.e. the percentage of times the SSE does not exceed the $\chi^2$threshold during the first detection step, when one or multiple faults are introduced. A larger bias leads to higher residuals what allows a better detection, as it is confirmed by the results. The introduction of 2 biases decreases the missed detection rate too. It has to be noticed that the absolute values obtained here are not the focusing points, because they are dependent of the false alarm parameter. What is important is the evolution of the missed detection rate with respect to others parameters. The evolution is not linear with respect to the number of satellite but it highly rises with the diminution of satellite number. This highlights the difficulty to use such algorithm in urban areas where few satellites are in view.

| Bias amplitude | Number of Satellites | | | |
|---|---|---|---|---|
| | 8 | 7 | 6 | 5 |
| 15 m | 4.50% | 13.19% | 18.14% | 38.43% |
| 30 m | 0.56% | 2.12% | 5.10% | 21.37% |
| 45 m | 0.27% | 0.75% | 2.69% | 13.97% |

Table 2: Missed Detection rate of the RAIM algorithm for 1 fault

After analyzing the detection performance of the RAIM algorithm, it is important to look at the identification performance, because the ability to keep using healthy satellite in hard conditions is a crucial issue for urban localisation. Let remind that the used identification algorithm is intentionally not iterative, and does not go back on the previous identification step if the new position is still unhealthy. Table 4 and Table 5 shows the false identification rate, i.e. the percentage of times a pseudoranges was identified as faulty, whereas it is not. Because 5 satellites do not allow an identification step, and 6 satellites allow the identification of only one fault, no results are presented for the non-corresponding cases.

| Bias amplitude | Number of Satellites | | | |
|---|---|---|---|---|
| | 8 | 7 | 6 | 5 |
| 15 m | 0.71% | 1.71% | 3.83% | 9.89% |
| 30 m | 0.06% | 0.32% | 1.23% | 5.55% |
| 45 m | 0.02% | 0.08% | 0.54% | 3.83% |

Table 3: Missed Detection rate of the RAIM algorithm for 2 simultaneous faults

| Bias amplitude | Number of Satellites | | | |
|---|---|---|---|---|
| | 8 | 7 | 6 | 5 |
| 15 m | 3.20% | 10.05% | 28.71% | - |
| 30 m | 0.84% | 4.41% | 19.17% | - |
| 45 m | 0.45% | 2.26% | 14.40% | - |

Table 4: False Identification rate of the RAIM algorithm for 1 fault

The missed identification rate, shown in Table 6 and Table 7, i.e. the percentage of faulty measurements which are not identified, presents similarities with the false identification rates. In the one fault case, the false and missed identification rates decrease with higher bias amplitude and with higher number of satellites. Indeed higher amplitude bias and higher redundancy cause more relevant residuals, less spread by matrix $S$.

| Bias amplitude | Number of Satellites | | | |
|---|---|---|---|---|
| | 8 | 7 | 6 | 5 |
| 15 m | 41.57% | 55.98% | - | - |
| 30 m | 43.91% | 56.18% | - | - |
| 45 m | 44.54% | 55.63% | - | - |

Table 5: False Identification rate of the RAIM algorithm for 2 simultaneous faults

Contrary to the missed detection rate, the false and missed identification rates rise considerably with the 2 simultaneous biases case. The presence of two faults makes the residuals less relevant, and the identification step less efficient. A simple example makes it easy to understand. The Figure 7 illustrates a virtual satellite configurations where four satellites are on the West to East axis, two faulty satellites at the South (with PRN 4 and 17), and one satellite at the North (with PRN 31). The latitude of the receiver is mainly determined by satellites 4, 17 and 31 because of the satellite configuration. Faults of similar amplitude on satellites 4 and 17 cause a bias on the receiver latitude estimation, then the satellite 31 seems to be faulty. Even if this is an extreme case, two biases can easily "blame" another satellite in function of their respective configuration. This explains partially the difficulty to identify faulty satellites in presence of multiple faults.

| Bias amplitude | Number of Satellites | | | |
|---|---|---|---|---|
| | 8 | 7 | 6 | 5 |
| 15 m | 7.52% | 21.38% | 41.64% | - |
| 30 m | 1.36% | 6.34% | 23.29% | - |
| 45 m | 0.68% | 2.89% | 16.70% | - |

Table 6: Missed Identification rate of the RAIM algorithm for 1 fault

| Bias amplitude | Number of Satellites | | | |
|---|---|---|---|---|
| | 8 | 7 | 6 | 5 |
| 15 m | 50.66% | 69.16% | - | - |
| 30 m | 40.58% | 61.21% | - | - |
| 45 m | 37.05% | 58.28% | - | - |

Table 7: Missed Identification rate of the RAIM algorithm for 2 simultaneous faults

It has to be noticed that the missed detection rate decreases with the bias amplitude whereas no influence is observed on the false identification rate. The explanation comes from analyzing the identification sequence. The probability to detect the presence of a fault after removing a 45m bias is higher than after removing a 15m bias. The additional detections lead to additional identifications divided between good detections and false alarms in the same proportion as before. This leads to decrease the missed identification rate and does not change the false detection rate.

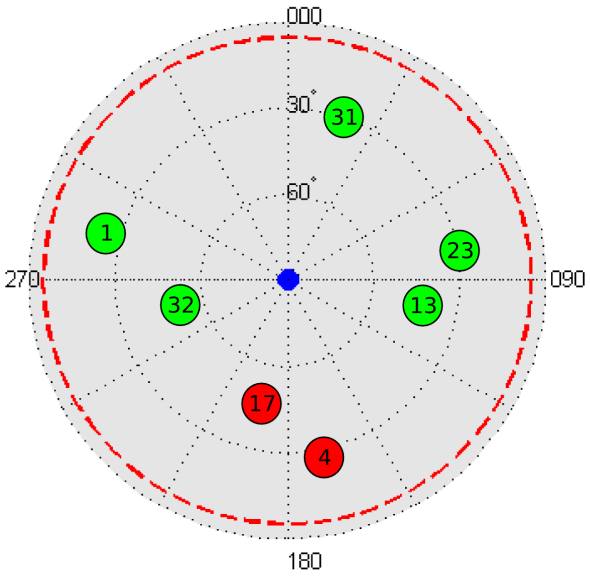


Figure 7: Virtual GPS constellation with two faults

Hence again, the interesting point is not the absolute values, but the difference between the one fault case, and the two faults case, as it is highly probable in urban environments with low-cost receivers.

### 5.2. KALMAN FILTER BASED FDE

Similar tests have been performed with the algorithm proposed in section 3.2. The false alarm rate used in the $\chi^2$test is the same as in the RAIM algorithm, but new tests have been added with a higher number of faults, and less satellites in order to emphasize the performance gain. Thus, tests have been performed with only 4 satellites and with 3 simultaneous biases for 7 and 6 satellites.

Because detection take advantage of the Kalman filter variables, the false detection rate is depending on the number and the amplitude of previously encountered faults. The Table 8 shows the false detection rate obtained with bias amplitude of 15 meters. As intended this rate increases with the fall of the satellites number. The performance gain obtained with bias of 30 and 45 metres does not exceed a factor of 2. Further analysis indicates that false detection mainly occurred when the Kalman filter state has an important error, superior to 50 meters. This is one of the main drawbacks of this algorithm: if the estimated state drifts because of undetected faults, or not enough accurate GPS positions, it can lead to detect non-existing faults. However, excluding healthy satellites just increases the uncertainty on the position but does not reduce integrity.

The missed detection rate is presented in Table 9. These results are significantly better than those obtained with the RAIM algorithm. The precision acquired during healthy periods enables a very sensitive detection of incoming faults, what avoids spoiling the state and keeps the detectability.

The ability to keep a good detection rate is related to

| Bias amplitude | Number of Satellites | | | | |
|---|---|---|---|---|---|
| | 8 | 7 | 6 | 5 | 4 |
| 0 | 0,00% | 0.00% | 1.42% | 3.23% | 6.21% |
| 1 | 0.01% | 0.55% | 1.03% | 3.06% | 6.61% |
| 2 | 0.03% | 0.06% | 1.00% | 3.37% | 10.13% |
| 3 | - | 0.10% | 1.51% | - | - |

Table 8: False detection rate of the Kalman Filter based FDE with a bias of 15 meters

| Bias amplitude | Number of Satellites | | | | |
|---|---|---|---|---|---|
| | 8 | 7 | 6 | 5 | 4 |
| 1 | 0.04% | 0.02% | 0.08% | 0.20% | 0.85% |
| 2 | 0.00% | 0.00% | 0.00% | 0.03% | 0.09% |
| 3 | - | 0.00% | 0.00% | - | - |

Table 9: Missed detection rate of the Kalman filter based FDE with a bias of 15 meters

good identification abilities. The false and missed identification rates are shown in Table 10 and Table 11, and confirm the performance gain regarding to the usual RAIM algorithm. As for the detection performance, the identification one is increased in the same proportion with bias of amplitude equal to 30 and 45 meters. An interesting point comes with a more precise analysis of the results: faulty satellites are more easily excluded if they are placed on the moving axis of the vehicle. Indeed, it is well known that the use of a Kalman filter with proprioceptive sensors flattens the uncertainty ellipsoid on the position, according to the moving axis of the vehicle. Then the use of this flattened covariance to compute the residuals gives such property to the detection and the identification.

| Bias amplitude | Number of Satellites | | | | |
|---|---|---|---|---|---|
| | 8 | 7 | 6 | 5 | 4 |
| 1 | 0,00% | 1,42% | 1,78% | 5,19% | 4,88% |
| 2 | 0,00% | 0,04% | 0,56% | 1,76% | 2,22% |
| 3 | - | 0,01% | 0,35% | - | - |

Table 10: False identification rate of the Kalman filter based FDE with a bias of 15 meters

## 6. CONCLUSIONS

Integrity associated to location estimates in the automotive domain is very specific and thus different to what is applied elsewhere. A novel algorithm capable of handling multiple faults and taking advantage of information from proprioceptive sensors in land vehicles has been proposed in this paper. To assess the capabilities of the new algorithm, its response was compared with that of a conventional RAIM type algorithm. For this purpose both algorithms were run using hybrid simulation techniques that provide relevant data. This includes the use of data from low-cost GPS receivers and the effects of an urban setting, plus vehicle ego-state information.

| Bias amplitude | Number of Satellites | | | | |
|---|---|---|---|---|---|
| | 8 | 7 | 6 | 5 | 4 |
| 1 | 0.04% | 0.02% | 0.14% | 0.53% | 1.77% |
| 2 | 0.05% | 0.07% | 0.18% | 0.80% | 3.32% |
| 3 | - | 0.14% | 0.45% | - | - |

Table 11: Missed identification rate of the Kalman filter based FDE with a bias of 15 meters

Results have shown the difficulties of the RAIM algorithm when confronted to multiple faults and poor satellite configurations, whereas the proposed algorithm showed a promising advantage. Its missed and false detection rates are significantly lower than that of a RAIM algorithm. Further studies should allow for a better simulation of GNSS satellite configurations in urban settings, particularly faults and receiver noise. Correlated faults, like tropospheric perturbations were excluded from due to their complexity, this needs to be studied further. Finally, the reduction of its performance as the Kalman filter state-error increases has to be addressed.

## REFERENCES


[1] S. Feng, W Ochieng, Integrity of navigation system for road transport, Proc. 14th World Congress of Intelligent Transportation Systems, Beijing, October 2007

[2] J. Cosmen-Schortmann and M.A. Martinez-Olagüe, GNSS based electronic toll collection system of guaranteed performances, Proc. 14th World Congress of Intelligent Transportation Systems, Beijing, October 2007

[3] B. Roturier, E. Chatre and J. Ventura-Traveset, The SBAS integrity concept standardised by ICAO: Application to EGNOS. The Journal of Navigation, Vol.49, no196, pp.65-77, 2001

[4] M. S. Grewal, L. R. Weill and A. P. Andrews. Global Positionning Systems, Inertial Navigation, and Integration. John Wiley and Sons, 2001.

[5] P.B. Ober, SBAS Integrity Concept, Technical Report 0.882, European Organisation for the Safety of Air Navigation, May 2001.

[6] T. Walter and P. Enge. Weighted RAIM for precision approach, in Proc. 8th International Technical Meeting of the Satellite Division of the Institute of Navigation, Palm Springs, CA, September 1995.

[7] S. Hewitson and J. Wang, GNSS Receiver Autonomous Integrity Monitoring (RAIM) Performances Analysis, GPS Solutions, Vol 10, pp. 155-170, 2006

[8] I. Martini, and GW. Hein, An Integrity Monitoring Technique for Multiple Failures Detection, in Proc. IEEE/ION PLANS, San Diego, April 2006.

[9] B. Belabbas and F.Gass, RAIM algorithms analysis for a combined GPS/Galileo constellation. Proc. ION GNSS, Long Beach, USA, 13-16 september 2005.

[10] Ph. Bonnifait, P. Bouron, D. Meizel, and P. Crubillé, Data fusion of four ABS sensors and GPS for an enhanced localization of car-like vehicles, in Proc. IEEE International Conference on Robotics and Automation (ICRA). Séoul, May 2001.

[11] Gao, J. M.G. Petovello and M.E. Cannon, Development of Precise GPS/INS/Wheel Speed Sensor/Yaw Rate Sensor Integrated Vehicular Positioning System. Proc. of ION NTM, Monterey, CA, Jan 2006.

[12] B. Liu, M. Adams and J. Ibanez-Guzmán, Multi-aided Inertial Navigation for Ground Vehicles in Outdoor Uneven Environments, Proc. IEEE International Conference on Robotics and Automation (ICRA), Barcelona, April 2005.

[13] S. Hewitson and J. Wang, GNSS receiver autonomous integrity monitoring with a dynamic model. The Journal of Navigation, Vol.60, pp. 247-263, 2007.

[14] P. B. Ober, New, Generally Applicably Metrics for RAIM/AAIM Integrity Monitoring, in Proc. 8th International Technical Meeting of The Satellite Division of The Institute of Navigation, Kansas City, USA, 17-20 September 1996.